

A Full Loss Cone for Triaxial Galaxies

K. Holley-Bockelmann,^{1,2*} & S. Sigurdsson^{1,2†}

¹ *Department of Astronomy, Pennsylvania State University*

² *Center for Gravitational Wave Physics, Pennsylvania State University, University Park, PA, 16802*

ABSTRACT

Stars and compact objects that plunge toward a black hole are either 1) captured, emitting gravitational waves as the orbit decays, 2) tidally disrupted, leaving a disc of baryonic material, 3) scattered to a large radius, where they may thereafter avoid encounters with the black hole or 4) swallowed whole, contributing to black hole growth. These processes occur on a dynamical time, which implies that for a static spherically symmetric stellar system, the loss cone is quickly emptied. However, most elliptical galaxies and spiral bulges are thought to be triaxial in shape. The centrophilic orbits comprising the backbone of a triaxial galaxy have been suggested as one way to keep the loss cone around a supermassive black hole filled with stars, stellar remnants, and intermediate mass black holes. We investigate the evolution of the loss cone population in a triaxial galaxy model with high resolution N-body simulations. We find that enough regular orbits flow through angular momentum space to maintain a full loss cone for a Hubble time. This increases the astrophysical capture rate by several orders of magnitude; we derive new capture rates for the Milky Way bulge and a triaxial M32-analogue. In the Milky Way, for example, we find that the white dwarf capture rate can be as high as 10^{-5} per year, 100 times larger than previous estimates based on spherical models for the bulge. This is the first step in a multiphase project that will explore the dynamics of supermassive black holes in realistic, fully self-consistent systems. The phase space content and time evolution of the loss cone affects supermassive black hole merger rates, extreme mass ratio inspiral rates, as well as the growth rate of a single supermassive black hole due to

stellar accretion, all key observables for the future Laser Interferometer Space Antenna (LISA).

Key words: galaxies: elliptical, galaxies: kinematics and dynamics, galaxies: structure, methods: n-body simulations

1 INTRODUCTION

Observations suggest that supermassive black holes are a part of nearly every galaxy center (e.g. Richstone et al. 1998), with masses ranging from $O(10^6)$ - $O(10^{10})M_\odot$. Gas accretion is thought to fuel the early stages of black hole growth, which may explain the tight correlation between black hole mass and the host galaxy’s global velocity dispersion (Gebhardt et al. 2000a; Ferrarese & Merritt 2000). Indeed, a supermassive black hole may be essential to regulate its host galaxy’s global structure and kinematics.

However, a single supermassive black hole (SMBH, hereafter) exacts a toll on its host galaxy, steepening the central cusp (Young 1980, Quinlan et al. 1995), and preferentially depleting the system of its low angular momentum material. Stars on plunging orbits interact with the SMBH and are removed from the galaxy by four basic processes:

(i) Tidal Disruption

A star is disrupted when it passes so close to the SMBH that the tidal force exerted by the SMBH exceeds the star’s own surface gravity. These stars are commonly thought to be the main source of the large amplitude X-ray outbursts seen in both active and inactive galactic nuclei (e.g. Donley et al. 2002) as the gaseous debris settles into an accretion disc and falls into the SMBH (e.g. Rees 1988, Bogdanovic et al. 2004). The tidal disruption radius, r_{tidal} depends on the stellar mass, radius, and internal structure:

$$r_{\text{tidal}} = \left(\frac{\eta^2 M_\bullet}{m_\star} \right)^{1/3} r_\star, \quad (1)$$

where $\eta \sim 2.21$ for an incompressible, homogeneous system, and $\eta = 0.844$ for a main sequence star modeled with a $n = 3$ polytrope (Magorrian & Tremaine 1999; Sridhar & Tremaine 1992, Diener et al. 1995). A G2V star would have to pass within 0.64 AU of the Milky Way SMBH to be disrupted, assuming the current best Milky Way SMBH mass estimate of $3.7 \times 10^6 M_\odot$ (Ghez et al. 2005).

* kellyhb@gravity.psu.edu

† steinn@astro.psu.edu

(ii) Swallow Directly

For high mass SMBHs, such that $M_{\bullet} > \sim 10^8 M_{\odot}$, the tidal disruption radius of a main sequence star can be smaller than the Schwarzschild radius, $r_{\bullet} = 2GM_{\bullet}/c^2$. In this case, stars plunge directly into the SMBH, possibly without any accompanying electromagnetic event. Since the tidal disruption radii of compact objects are much smaller, they can be swallowed whole by lower mass SMBHs as well: 10-30 % of the total flux of stellar objects into a $10^6 M_{\odot}$ SMBH can be attributed to compact objects and dark matter particles that have been swallowed whole (Zhao, Haehnelt & Rees 2002; though see Hopman & Alexander for a larger estimate).

(iii) Capture and Inspiral

Those objects that survive a close pericenter pass without disruption can be captured by the SMBH on a bound quasi-Keplerian orbit. Typically, this occurs when a white dwarf, neutron star or black hole (of any mass) passes within *few* – $100M_{\bullet}$ of the SMBH (in $c = G = 1$ units, i.e. 1.5 – 7.6 AU for the Milky Way SMBH)¹. This newly formed close binary has a large dynamic quadrupole potential and begins to emit significant gravitational radiation (Peters 1964) with a characteristic amplitude h :

$$h \sim 4 \times 10^{-24} \left(\frac{m_{\star}}{d}\right)^{1/3} \left(\frac{M_{\bullet}}{10^6}\right)^{2/3} \left(\frac{10^4}{P}\right)^{2/3}, \quad (2)$$

where the orbital period P is measured in seconds, the stellar remnant mass m_{\star} is measured in solar masses, and the distance to the source d is measured in Gpc. As a consequence of losing energy via gravitational radiation, the compact object spirals in and eventually coalesces with the SMBH. These extreme mass ratio inspirals (EMRIs) are a prime observational candidate for LISA, a planned gravitational wave telescope set to launch in 2017. Current estimates suggest that LISA will observe about one stellar mass EMRI per year within 1 Gpc of Earth (Hils and Bender 1995, Sigurdsson & Rees 1997, Sigurdsson 1998, Freitag 2003, Ivanov 2002, though see Hopman and Alexander 2005 for a significantly lower estimated rate of detection.)

(iv) Ejection

Interactions between stars can induce changes in each stellar velocity of the order:

$$\delta v_1 \sim 4.4 \times 10^2 \frac{\text{km}}{\text{s}} \left(\frac{2m_2}{m_1 + m_2}\right)^{\frac{1}{2}} \left(\frac{m_2}{1M_{\odot}}\right)^{\frac{1}{2}} \left(\frac{1R_{\odot}}{b}\right)^{\frac{1}{2}}, \quad (3)$$

where b is the impact parameter between the two stars, m_1 and m_2 are the masses of stars

¹ For this paper, we ignore captures from neutron stars

1 and 2, respectively (Yu & Tremaine 2003). It is quite rare to eject main sequence stars with a large enough velocity to escape the Milky Way entirely by this process, occurring less than once per Hubble time. However, if the two stars were bound as a binary, the SMBH can break the binary apart and eject one of the stars with $O(10^3)$ km/sec velocities (Hills 1988, Gould & Quillen 2003, Yu & Tremaine 2003). This process occurs more commonly for the Milky Way, at a rate of $10^{-5}(\eta/0.1)$ per year, where η is the binary fraction (Yu & Tremaine 2003).

Though we have described this 3-body removal process in terms of two stars and one SMBH, ejection is a much more efficient process when there are two black holes and one star. If there are two black holes of significant mass bound at the center of the Milky Way, either another lower mass SMBH or an intermediate mass black hole, then the number of stars that can be ejected is much larger, because stars need pass only within the separation between the two black holes to receive energy and angular momentum. Given a second SMBH with a mass much smaller than the first, Yu & Tremaine (2003) estimate the $O(10^{-4})$ stars are ejected per year, with as many as 1000 stars having ejection velocities $> 10^3$ km/sec inside the solar radius (see also Mapelli et al. 2005).

Since stars are lost from the system by these 4 processes, they comprise the 'loss cone' of the galaxy.² The loss cone is rapidly depleted of its stellar reservoir in at most a few dynamical times. With a depletion timescale this rapid, it has become a puzzle to understand how the loss cone could be anything other than empty, overall. In a static, spherical galaxy model, for example, the loss cone can only be refilled by 2-body relaxation, as long as 3-body scattering ejects stars permanently (e.g. Milosavljević & Merritt 2003). Because the timescale for refilling the loss cone via 2-body relaxation can be much longer than a Hubble time,

$$T_{\text{relax}} \sim 2 \times 10^9 \text{yr} \left(\frac{\sigma}{200/\text{km/sec}} \right)^3 \left(\frac{\rho}{10^6/M_{\odot}/\text{pc}^3} \right)^{-1}, \quad (4)$$

the loss cone remains empty over a galaxy lifetime; this will render any type of stellar interaction with a SMBH very inefficient, at least in static, spherical models.

Filling a loss cone, relies on maintaining a reservoir of low angular momentum stars within

² Traditionally, the term 'loss cone' has referred only to the tidal disruption process. We have settled on a broader definition. Tidal disruption is the dominant process for main sequence stars interacting with a Milky Way-scale SMBH, while captures are by far the dominant processes for compact objects such as white dwarfs, neutron stars and up to intermediate mass black holes.

the galaxy, so considering more realistic galaxy shapes may be the key. While most loss cone studies have concentrated on static, spherical galaxy models, theory and observations both indicate that dark matter halos and elliptical galaxies are at least mildly triaxial (Bak & Statler 2000, Franx, Illingworth, & de Zeeuw 1991). Triaxiality is present not only elliptical galaxies, but in disc galaxies as well: a barred galaxy is a prime example of a rotating triaxial ellipsoid, which has a more complex orbital structure and response to a SMBH (Hasan & Norman 1990, Sellwood & Shen 2004). Over 70 percent of the local disc galaxy population is barred, and early indications suggest that this fraction may stay constant out to redshift 1 (Jogee et al. 2004; Sheth et al. 2004). Our own galaxy hosts a bar with a semi-major axis length of about 2 kpc seen nearly end on from our perspective ($\phi_{\odot-\text{bar}} \sim 20^\circ$; see Gerhard 2001 for a review).

Non-axisymmetry can introduce more stars to the loss cone in several ways. First, stars in even a mildly triaxial potential move in entirely different orbit families than are present in a spheroid (see Figure 1). In particular, there are a rich variety of regular box and boxlet orbits that are centrophilic and comprise the backbone of the galaxy (Miralda-Escude & Schwarzschild 1989). These centrophilic orbits can pass formally through, or very near to the SMBH, which make them the primary regular orbital component of the loss cone in a non axisymmetric galaxy.

Besides the regular box and boxlet orbits, chaotic orbits often occur a triaxial galaxy. Though chaotic orbits are generically in a triaxial galaxy, they are particularly prevalent in one that is embedded with a SMBH. In fact, it is a commonly thought that SMBHs cannot exist in a stable triaxial galaxy, because black holes induce chaos in the centrophilic orbit families (Norman, May & van Albada 1985, Gerhard & Binney 1985, Miralda-Escude & Schwarzschild 1989, Merritt & Quinlan 1998, Valluri & Merritt 1998, Holley-Bockelmann et al. 2002, Poon & Merritt 2002). and drive the galaxy toward axisymmetry in a few crossing times. Fully self-consistent, high resolution n-body simulations show, however, that triaxiality is not entirely destroyed by a SMBH. Though SMBHs do indeed incite chaos in box and boxlet orbits at small radii and do rounden the region inside the radius of influence $r_{\text{inf}} \equiv GM_{\bullet}/\sigma^2$, most of the centrophilic orbits are simply scattered onto resonant (or sticky) orbits that allow triaxiality to persist over most of the galaxy for many Hubble times (Holley-Bockelmann et al. 2002; see also Poon & Merritt 2002).

Due to their stochastic motion through phase space, chaotic orbits can refill the loss cone as well. Stars on chaotic orbits encounter the SMBH once per crossing time with a

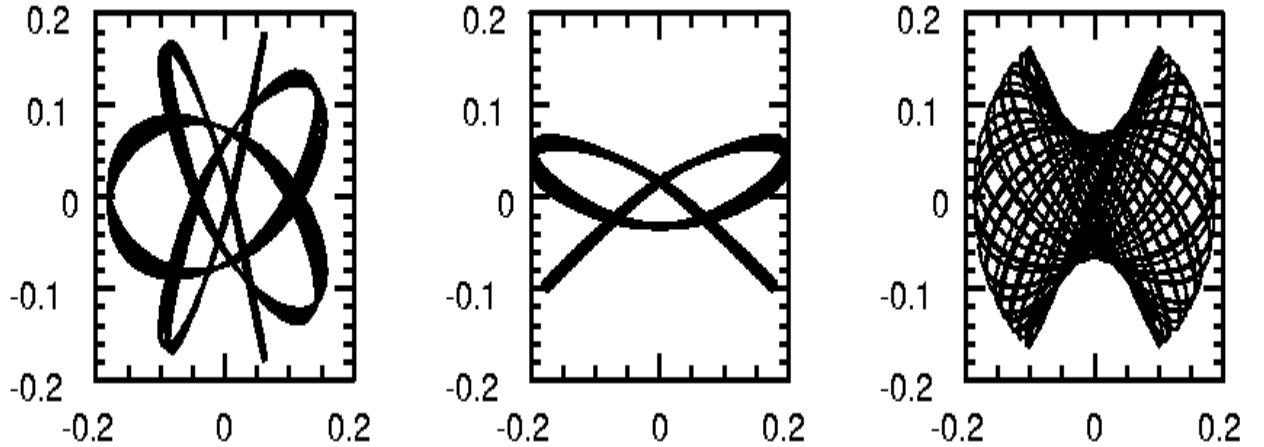


Figure 1. Planar Centrophilic orbits in a triaxial potential with no SMBH. The left panel is a resonant 7:6 boxlet, the middle panel is a 4:3 resonant boxlet (a.k.a. pretzel), and the right panel is a non-resonant box. These orbits will pass through the center of the potential. The box orbit, in fact, has no net angular momentum and can pass formally through zero. In general, angular momentum is not conserved for any orbit in a triaxial potential.

pericenter separation that varies each time, eventually passing close enough to the SMBH to be captured or tidally disrupted. Merritt & Poon (2004) showed that, for triaxial models where the fraction of chaotic orbits is substantial ($\sim 50\%$), the capture rate deep inside the sphere of influence of the SMBH meets and even exceeds that of a full loss cone for a spherical isotropic model. Lower energy orbits, however, experience a capture rate several orders of magnitude lower than a full spherical loss cone. Despite its efficiency close to the black hole, it requires a chaotic orbit fraction that may not exist in real galaxies or in N-body generated models (Holley-Bockelmann et al. 2002).

In this paper we investigate a new loss cone refilling mechanism, uniquely present in any non-axisymmetric galaxy. Since orbits in a triaxial potential do not conserve angular momentum, stars can stream rapidly through angular momentum space. This organized flow can occur for any orbit, regular or chaotic, as a consequence of the lack of symmetry in the system which prevents angular momentum from being a constant of the motion. Since any star can flow through angular momentum space, it can be a highly efficient means of transporting stars through zero angular momentum. Even if only a very small fraction of these stars are present in the loss cone, it may be enough to keep it filled.

Since most galaxies are so far from spherical, it is important to determine how more realistic galaxy models effect the structure and time evolution of the loss cone. This is the first paper in a series that will investigate the behavior of the loss cone in general for non-spherical

galaxies. Here, we quantify how angular momentum flow refills the 'capture and inspiral' loss cone in a triaxial potential and allows compact objects to be more efficiently captured onto orbits that emit significant gravitational radiation. We demonstrate this mechanism in section 3 and determine the fraction of orbits that can stochastically participate in refilling the capture and inspiral loss cone in an N-body generated triaxial galaxy model. We also explore the astrophysical consequences of this angular momentum flow on the EMRI rate, the SMBH growth rate, and the final parsec problem in sections 4-6. We find that this process alone can replenish the capture and inspiral loss cone as fast as it empties, resulting in an EMRI rate in the Milky Way that is 100 times larger than the canonical estimate for a spherical, isotropic Milky Way bulge model.

Though we first consider angular momentum flow for all orbits in a triaxial potential, more traditionally diffusive processes can refill a loss cone as well. We include dynamical friction (the first order Fokker-Planck term) and 'kicks' (2nd-order Fokker-Planck diffusion) using a hybrid SCF/Fokker-Planck code in our next paper. We are also generating a live 10^7 particle triaxial model to study the time-dependent, non-equilibrium loss cone refilling rate, and we are using these models to explore the decay of binary supermassive black holes explicitly.

2 NUMERICAL TECHNIQUES

Most previous studies of the loss cone have assumed that the typical change in angular momentum is small compared to the total angular momentum. Assuming $\Delta J \ll J$ allows a Fokker-Planck or perturbative approach to the loss cone problem (Cohn & Kulsrud 1978; Magorrian & Tremaine 1999; Hopman & Alexander 2005). This is useful to track diffusion via 2-body scattering or chaotic diffusion, but is not an accurate way to track the potentially large changes in angular momentum that may occur from this angular momentum flow.

We have decided to use n-body simulations as a testbed to quantify the angular momentum flow. We compare two n-body generated systems with the same final density profile and same black hole mass, but very different shapes, one spherical and one with a varying triaxiality from the center out, and we track the amount of angular momentum flow per orbit for each system. The procedure for generating these models is outlined in Holley-Bockelmann et al. 2001 and Holley-Bockelmann et al. 2002; we review it briefly here. The advantage of this

technique is that by using models with the same density profile and same n-body generation technique, we can isolate the effect of angular momentum flow has on a preexisting loss cone.

We begin with an 512,000 particle equilibrium spherical Hernquist model populated with a multimass scheme, so that a particle has a mass that is roughly inversely proportional to its pericentric radius. We use a parallel version of the self-consistent field (SCF) basis expansion code with multiple timesteps and a 4th order Hermite integrator to adiabatically squeeze the spherical model into a mildly triaxial one, then adiabatically grow a SMBH at the center of the potential (see Holley-Bockelmann et al. 2001; Holley-Bockelmann et al. 2002 for more details on the technique and model parameters). We keep all terms in the basis expansion to $(n, l) = 12, 8$. This SMBH-embedded model model has a triaxiality that varies from $a : b : c = 1.0 : 0.95 : 0.92$ inside r_\bullet to $a : b : c = 1.0 : 0.85 : 0.7$ at the effective radius.

To isolate the effect of the different orbit content and integrals of motion in the triaxial system, we froze the potential of our triaxial model and followed the orbits for a Hubble time, tracking the change in angular momentum, pericenter distance, orbital period, eccentricity, relaxation time and other orbital parameters. We conducted the same experiment using a SMBH-embedded spherical Hernquist model as a control. To decrease the spatial potential fluctuations, we took advantage of the 8-fold symmetry of our static models to seed the final potential with mirror particles (see Holley-Bockelmann et al. 2001, 2002 for more details), giving the models the equivalent Poisson noise of a 4 million particle system.

3 RESHUFFLING THE LOSS CONE

In this section, review some of the processes that change the orbits within the loss cone and describe the how the loss cone reservoir can be reshuffled when orbits do not conserve angular momentum.

First, a few cautionary notes: First, when discussing the loss cone, there are often references to two regimes, 'diffusion' and 'pinhole'. The 'pinhole' regime where the loss cone width is small compared to ΔJ , and in a spherical galaxy this dominates at larger distances from the SMBH. Closer in, where the loss cone width is larger, is the 'diffusion' regime; here the typical orbit has ΔJ smaller than the loss cone width. However, these definitions are insufficient, and even inaccurate, for processes that allow the orbits to change angular momentum by large amounts. In that case, the 'pinhole' regime could dominate all the way to the black hole for some types of orbits and not others. For this reason, we decided not

to define this angular momentum flow in terms of whether it acts in the pinhole regime or not. In fact, we use this terminology sparingly. Instead, we simply quantify how many orbits stream through angular momentum space and how quickly they do so as a function of radius.

Second, in our models, we neither adjust the trajectories of inspiralling particles as they begin to emit gravitational radiation nor do we extract particles from a loss cone when it enters. It is not necessary to make this adjustment because with only 512000 particles, the number of particles within the loss cone is zero. In fact, at any given time, a galaxy with the mass of the Milky Way has zero occupancy within the loss cone, i.e. integrating the distribution function over this region of phase space indicates that expected number of stars within the loss cone is less than 1. The orbits which meet the low angular momentum criteria are both extremely rare and will interact with the SMBH very quickly, thus removing them from the system. This occurs even for a full loss cone. So, with essentially zero occupation in the loss cone, we follow the analytic prescriptions of Frank & Rees (1976) and Sigurdsson & Rees (1997) to define the capture and inspiral loss cone as the region in angular momentum space where an orbit decays via gravitational radiation much faster than its relaxation time, $T_{\text{gw}} < T_{\text{relax}}$.

If we take the Frank and Rees (1976) approach and define the dimensionless angle, $\theta(r) = \sqrt{2r_{\text{min}}/3r}$, loosely associated with the eccentricity of an orbit, the rate at which stars are captured by two-body relaxation or large-angle scattering is:

$$R_s = \frac{N_\star(r)^2 \theta_{\text{crit}}^2 m_\star^2}{M_\bullet T_{\text{orb}}}, \tag{5}$$

where θ_{crit} for two-body relaxation is:

$$\theta_{\text{crit}} = \sqrt{\frac{3}{2}} \left(\frac{85\pi}{24\sqrt{2}} \right)^{1/5} \left[\frac{M_\bullet}{m_\star N_\star(r)} \right]^{1/5} \left(\frac{r}{r_s} \right)^{-1/2}. \tag{6}$$

And θ for large angle scattering is:

$$\theta_{\text{crit}} = \sqrt{\frac{3}{2}} \left(\frac{85\pi}{24\sqrt{2}} \right)^{1/7} \left[\frac{M_\bullet}{m_\star N_\star(r)} \right]^{1/7} \left(\frac{r}{r_s} \right)^{-5/14}. \tag{7}$$

The current level of discreteness noise in a $O(10^6)$ particle N-body simulation overestimates the degree of two-body relaxation and underestimates the number of large angle scatterings in a galaxy, so it would be inaccurate to identify the rate of depletion via these two process directly from our models. We plan on studying these processes directly in a time-dependent N-body simulation with better resolution, in the future. Here, we determined the

width of the cone, θ , that each of these two-body processes subtend within the phase space of our model, and determined the rate of depletion from that area as defined in equation 5.

Even in the absence of two-body relaxation and large angle scattering, orbits in a triaxial potential stream about in angular momentum as they obey different integrals of motion (see figure 2). This 'reshuffles' phase space and systematically introduces new orbits into the loss cone. Once an orbit is inside the loss cone, its apocenter shrinks rapidly, so flow *out* of the loss cone via this process is much slower than the flow in.

An orbit has completely changed its angular momentum when $\Delta J/J_{\text{init}} = 1$. Figure 2 shows that, in total, about 0.2% of the orbits in our model change their angular momenta by order unity in merely 1000 dynamical times, or 4.5×10^7 years at r_{inf} for a system scaled to the Milky Way. In figure 3, we demonstrate how quickly each orbit reshuffles its angular momentum per dynamical time: $\Delta J/J_{\text{init}}|_{t_{\text{dyn}}}$ for 4 regions of total energy in the model.

For each particle in our simulation, we calculate the time it would take to change angular momentum by order unity, $t_{\text{reshuffle}}$. We determine this directly from the change in angular momentum per dynamical time for each orbit within the frozen triaxial potential. By keeping track of the how rapidly each orbits flows through phase space, we can estimate the rate any particular loss cone is refilled due to this process alone:

$$R_{\text{reshuffle}} = \frac{N(r)}{t_{\text{reshuffle}}}, \quad (8)$$

where $t_{\text{reshuffle}}$ is:

$$t_{\text{reshuffle}} = \frac{J_{\text{init}}}{\Delta J} \Big|_{t_{\text{dyn}}} t_{\text{dyn}} \left[1 - \theta_{\text{crit}}^2 \right]. \quad (9)$$

Note that if a model had equal-mass particles, $N(r)$ would be a sum over the number of particles found in a radial bin. However, recall that we generated our numerical model with a 'multimass' technique (see Sigurdsson et al 1998; Holley-Bockelmann et al. 2001), assigning more particles with smaller individual masses to the center. These different masses change the weight of each individual particle in the rate estimate, making $N(r) = \sum_{i=1}^n m(i)/M(r)$, where $M(r)$ is the mass of the model at radius r and $m(i)$ is the particle mass. Since this equation simply records how long a particular orbit takes to completely scramble its angular momentum, it holds for any density profile, any galaxy shape, and any type of orbit. In fact, in the trivial case of one star moving in a closed orbit about a point mass, $t_{\text{reshuffle}}$ is infinite.

Figure 4 shows the rate of flow into the capture and inspiral loss cone for particles in the simulation under different processes. Note that the rate particles stream into the loss cone by this triaxial scrambling process is much larger than the rate in which they are lost by 2-

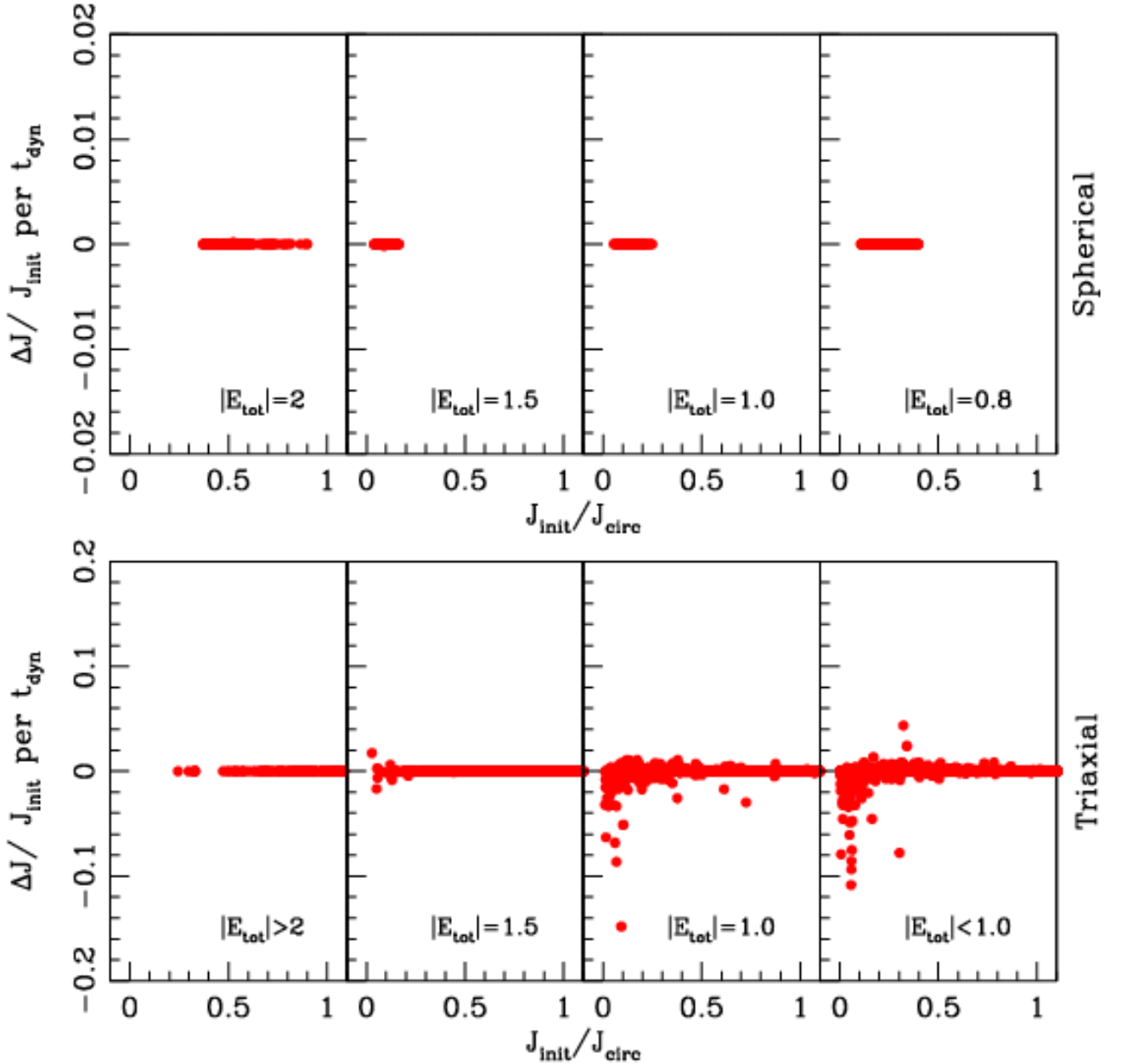


Figure 2. The change in the angular momentum per dynamical time as a function of the normalised angular momentum κ for several energies. The points represent all the orbits in our course-grained sample of the mass density. In the triaxial potential (bottom), many orbits change their total angular momenta significantly per dynamical time. Note the vertical scale for the spherical model (top) is 10 times smaller

body relaxation and large angle scattering combined. And, since technically every orbit can participate in reshuffling the phase space of the loss cone, we anticipate that the loss cone reservoir in a triaxial potential is always filled. Again, this is because there is a large amount of flow both in and out of the loss cone at large radii. Normally, this would be symmetric, but the SMBH provides a sink that captures an extremely small fraction of the orbits that just happen to be at the right phase, thereby keeping the loss cone full.

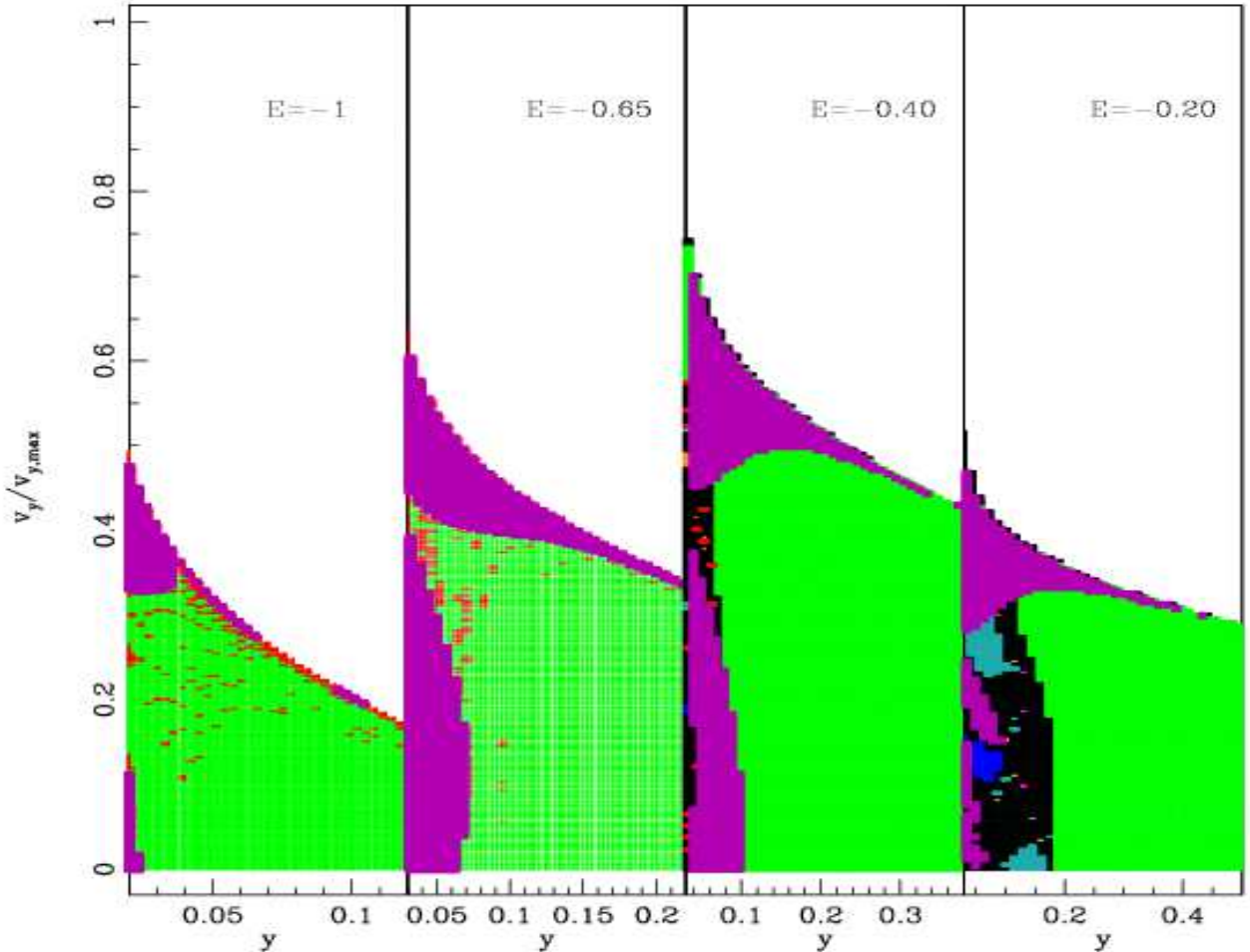


Figure 3. The surface of section for several energies. Different colors represent different orbit types. Red are chaotic orbits, black are boxes, blue are fish, cyan are pretzels, orange are 5:4 resonances. Overlaid in purple are the orbits that change angular momentum the most per dynamical time of a circular orbit at that energy (the top 10 percent in each energy bin are plotted). The orbits that typically move in angular momentum the most are boxes and chaotic orbits.

4 ASTROPHYSICAL CAPTURE RATE

In the previous section, we defined a capture and inspiral loss cone and showed that, in a triaxial potential, this region is everywhere full because orbits are capable of streaming through angular momentum space. The capture loss cone contains a smaller subset of particles with trajectories that slowly spiral into the black hole, which generate clean Extreme Mass Ratio Inspirals that LISA will detect. There is some indication that a significant fraction of stars within the capture loss cone may plunge into the SMBH so quickly that LISA will be unable to detect an inspiral signature (Hopman & Alexander 2005). This study, however, only considered diffusion in the pinhole regime, and it is likely that large angle scattering is critical in this part of the loss cone. Most studies have equated the

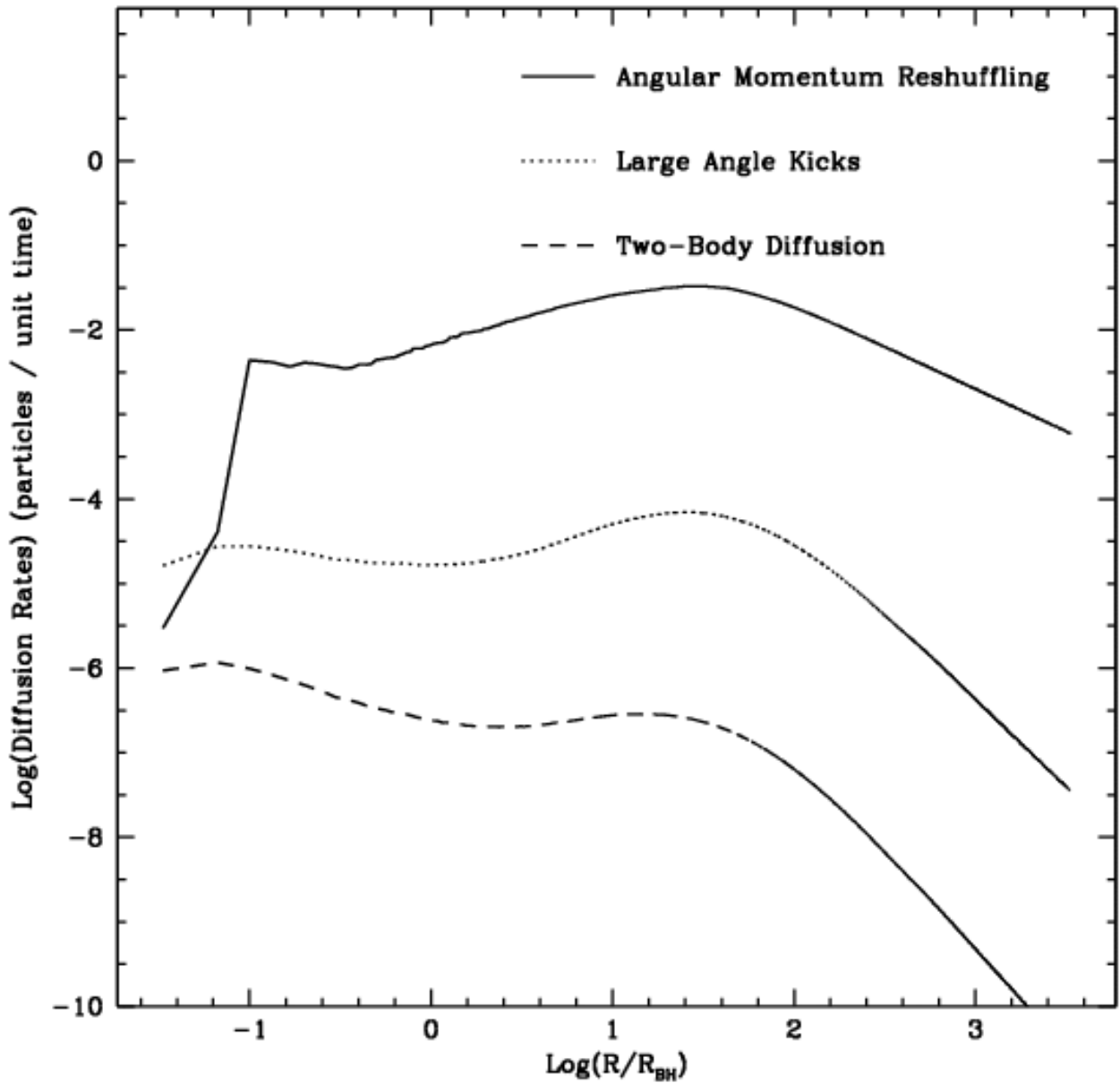


Figure 4. The rate of depletion and replenishment of the loss cone as a function of radius for all particles in the simulation in model units. Here, the particles trace the density coarsely, and each particle represents many stars. When scaled to the Milky Way bulge, the average particle in our simulation represents about $800M_{\odot}$, and the dynamical time at r_{BH} is $\sim 5 \times 10^4$ years.

astrophysical capture rate in the Milky Way and M32 to the LISA rate (within a factor of a few). We make the same assumption, but caution that the fraction of captures LISA can actually detect per galaxy may be small.

We can estimate the rate of capture for different compact object populations for a particular galaxy by converting the mass density of particles in our simulation into a number density of the compact objects of interest. To do this we assume that the mass density or our

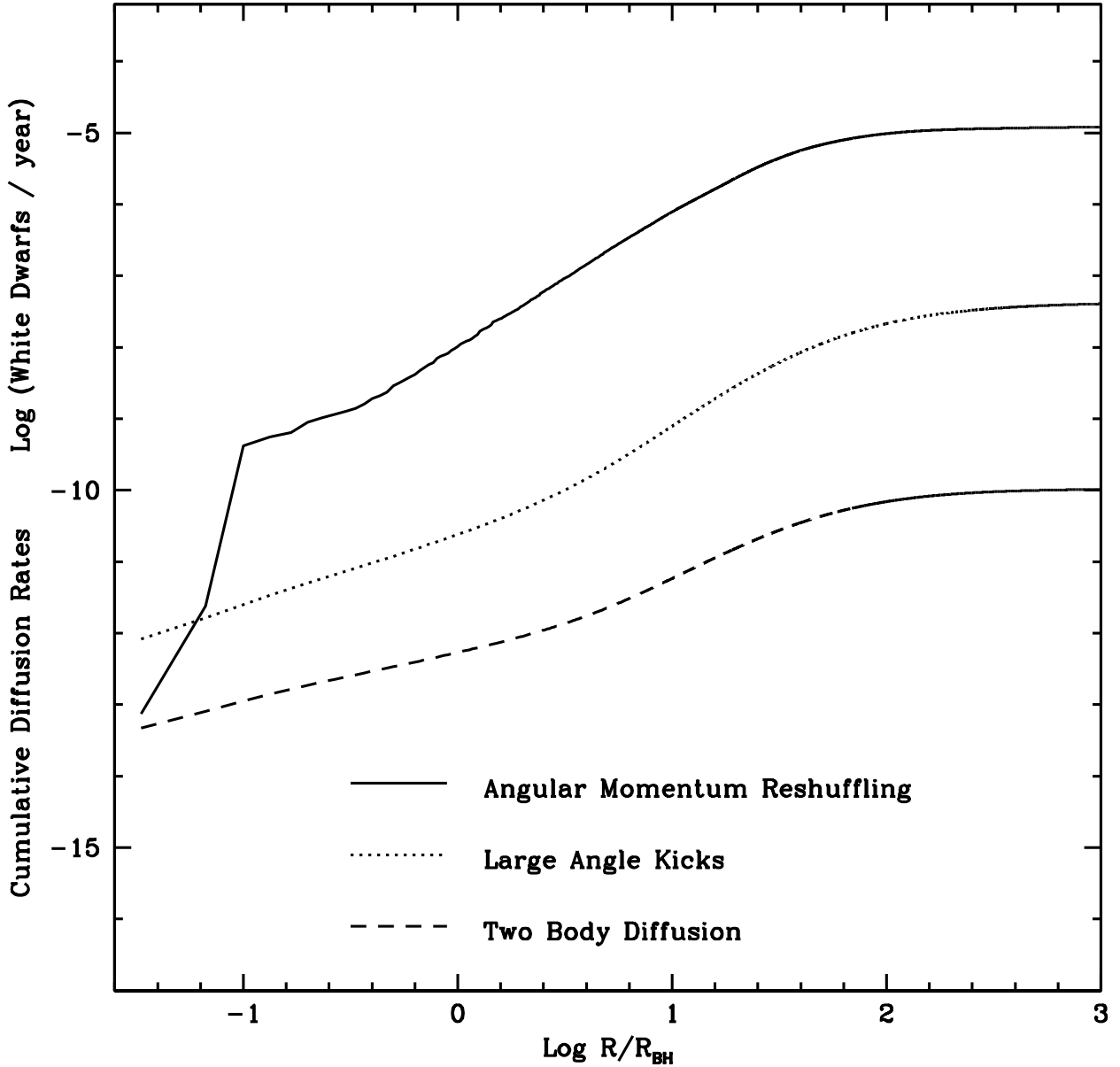


Figure 5. The cumulative rate of depletion and replenishment of the loss cone as a function of radius for white dwarfs when the model is scaled to the physical parameters of the Milky Way bulge. We assume the particle mass distribution of the simulation maps the smooth mass distribution of the galaxy model, and that all stars were formed in a single burst 10 Gyr ago with a Scalo IMF. White dwarfs are assumed to form from stars with initial masses between $1 - 8M_{\odot}$.

coarse-grained model maps the mass density of the galaxy, after scaling the size and total mass. We assume the mass density results from a single burst of star formation 10 Gyr ago, and that the number of stars per unit mass follows a Scalo IMF (Scalo 1986). We further assume that white dwarfs formed from all the stars between $1 - 8M_{\odot}$ and that stellar mass black holes formed from stars between $20 - 300M_{\odot}$. This calculation neglects the effects of mass segregation and multiple episodes of star formation, both of which should increase the

Table 1. Astrophysical Capture Rates and Physical Scaling

Galaxy Model	$M_{\bullet}(M_{\odot})$	$M_{\text{bulge}}(M_{\odot})$	Effective Radius (pc)	White Dwarf Captures (yr^{-1})	Black Hole Captures (yr^{-1})
M32	3×10^6	3×10^9	200	5×10^{-6}	9×10^{-9}
Milky Way bulge	3×10^6	2×10^{10}	2000	1×10^{-5}	2×10^{-7}

rate of low mass black hole captures significantly. Table 1 presents the white dwarf and stellar mass black hole capture rate for the Milky Way bulge and for M32, and figure 5 shows the cumulative rate of capture for white dwarfs in the Milky Way bar. We find that the total large angle scattering and diffusion capture rate for white dwarfs is $O(10^{-7})$ per year in the Milky Way bulge, consistent with previous work. The rate of captures from angular momentum reshuffling, however, is much larger: $O(10^{-5})$ white dwarfs per year. As a rough consistency check, if a the dynamical time of a typical capture orbit were 10^4 years, this capture rate suggests capture occurs once every 10 dynamical times at that energy, which would yield a reasonable occupation fraction of 10%; in other words, the flow only captures 10% of the available orbits with these parameters.

This rate is robust for this process only as well as our galaxy model matches the Milky Way inner regions. The most glaring difference is that a bar is a rotating triaxial ellipsoid, which hosts more chaotic orbits, but fewer real boxes. Consequently, it is not immediately clear how the rate should be adjusted to account for bulk rotation, but the capture rate in the Milky Way bar could change by an order of magnitude or more. We plan to study this with detailed N-body simulations in the future.

5 LISA SIGNALS FROM INTERMEDIATE MASS BLACK HOLE INSPIRALS

For each particle, we determined the gravitational wave signal during close encounters with the SMBH. Very near the SMBH, we can approximate the orbit as Keplerian; for this equivalent Keplerian orbit, the time to travel through the arc described by the latus rectum yields the frequency of interaction, while the eccentricity yields the power radiated in gravitational waves (Peters & Mathews 1963):

$$P = \frac{8}{15} \frac{G^4 m_1^2 M_{\bullet}^2 (m_1 + M_{\bullet})}{c^5 a^5 (1 - e^2)^5} (1 + e \cos \theta)^4 [12(1 + e \cos \theta)^2 + e^2 \sin^2 \theta]. \tag{10}$$

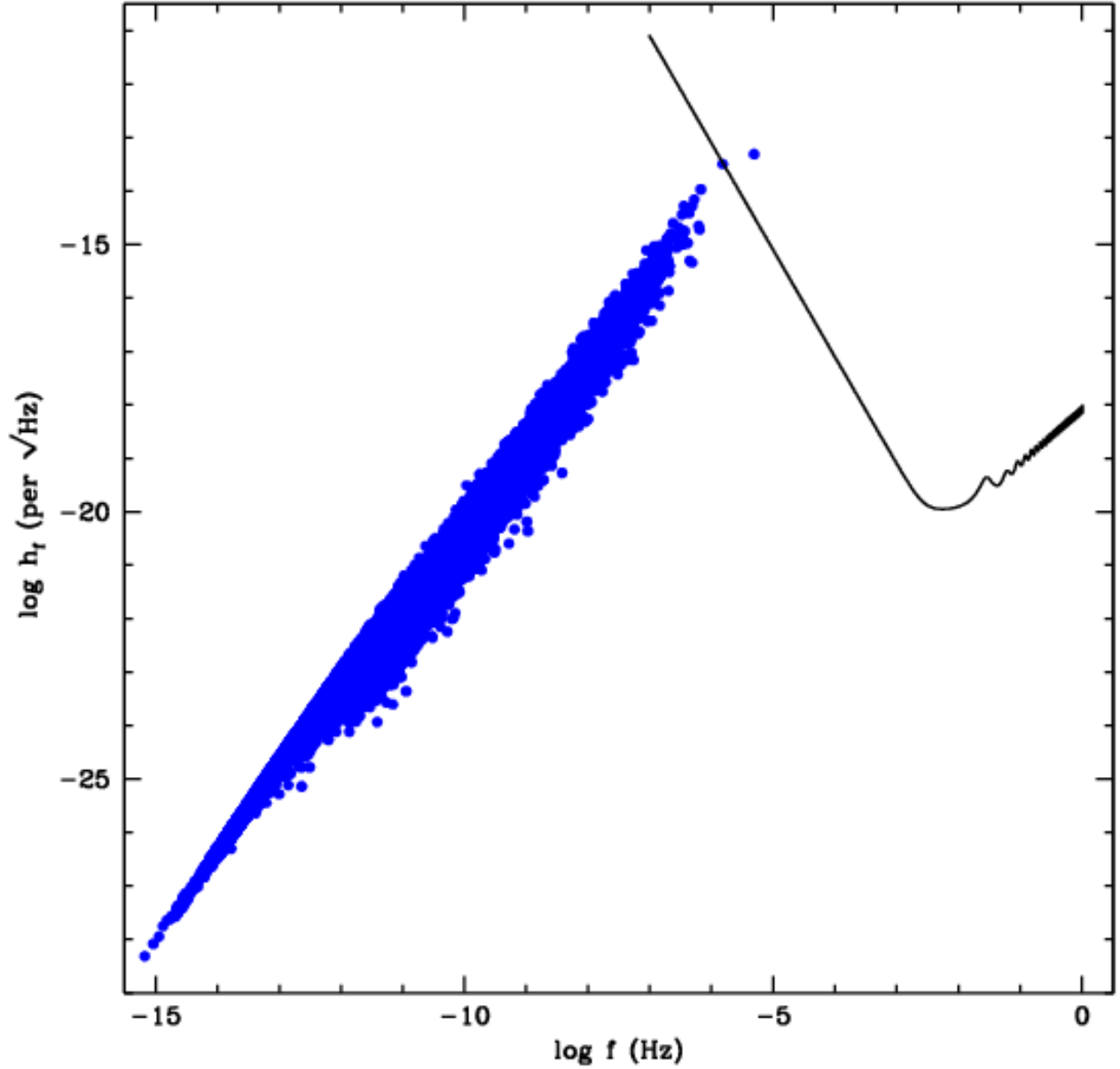


Figure 6. The estimated gravitational wave strength as particles pass pericenter in the simulation. The particles were scaled in mass such that the total mass is equal to the Milky Way bulge, so that each particle is approximately $800M_{\odot}$, and the strain is calculated assuming the SMBH is 8 kpc from the detector. Each simulation particle normally represents many stars, so any IMBH-SMBH rate inferred from this figure would be unphysical. However, if there were IMBHs in our Milky Way bulge, the centrophilic orbits in the bar would pass close enough to the SMBH to yield LISA burst signals.

The power is related to the strain amplitude in the following way:

$$h_f = \sqrt{\frac{4G}{16c^3\pi^2} \frac{P}{f_{\text{orb}}^2 D^2}}. \quad (11)$$

If we scale the model to the Milky Way bulge and allow the particle mass to set the mass of the interacting particle ($800M_{\odot}$), then our simulation produces two highly eccentric Intermediate Mass Black Hole (IMBH)-SMBH encounters with a signal to noise ratio of

approximately 1000 (Figure 6). These orbits pass by the SMBH with eccentricities > 0.99 , spending only 10^5 seconds to fly by the SMBH at pericenter distances of about 200 AU. This could be a relatively unexplored source of LISA burst signals, assuming that the spacecraft will have the expected sensitivity in the 10^{-5} Hz band. These encounters are more likely with a triaxial model, due to the increased fraction of centrophilic orbits, though this begs the question of how one produces an $O(10^3)M_\odot$ IMBH in the first place (Gebhardt et al. 2000b; Gerssen et al. 2003; Taniguchi et al. 2000, Miller & Hamilton 2002). However, even if these were more common $10 M_\odot$ stellar mass black holes, they would still produce a LISA burst signal as they pass through pericenter.

6 IMPLICATIONS FOR BINARY BLACK HOLE MERGERS

During a galaxy merger, each SMBH sinks to the center of the new galaxy potential due to dynamical friction and eventually becomes a bound SMBH binary (SMBBH). Dynamical friction still shrinks the SMBBH orbit until the binary is hard; thereafter, further decay is mediated by 3-body scattering with the ambient stellar background until the SMBBH becomes so close that the orbit can lose energy via gravitational wave emission, and the SMBBH can presumably coalesce.

The SMBBH loss cone is larger than for single SMBH, since stars must only pass within the separation a of the SMBBH, where $a = G(M_1 + M_2)/8\sigma_*^2 \sim 0.05$ parsec for two equal $10^6 M_\odot$ SMBHs. Unfortunately, once the SMBBH has interacted with all the stars within its loss cone, the orbit decay stalls within the center of the galaxy with a separation \sim parsec.

This is known as the 'final parsec problem': the orbit of a SMBBH in idealized galaxy models never decays enough to allow gravitational wave emission to drive the system to coalesce. The behavior of stars in angular momentum space is deeply connected to this problem, since an ample supply of low angular momentum stars is tantamount to providing a fresh reservoir of orbits within the loss cone.

Our results for the refilling rate of the capture and inspiral loss cone imply that it is always full. In other words, there are many more particles that can flow through the capture and inspiral loss cone than can be depleted by gravitational encounters. Hence in principle, the larger loss cone for 3-body scattering by a binary black hole can also remain full in a triaxial potential. We are developing a fully self-consistent n-body model with 10^7 particles

to explore the shape, time dependence, and phase space content of the SMBBH loss cone explicitly.

We note that our triaxial galaxy model was constructed from an equilibrium spherical potential; if SMBBH are formed as the byproduct of major galaxy mergers, they likely inhabit post-merger remnant galaxies that are significantly more flattened ($c/a = 0.7$ for our model versus $c/a = 0.4 - 0.6$ for the typical equal-mass merger remnant (Statler 2004)). We are determining how the loss cone refilling rate depends on the degree of flattening for a number of equilibrium triaxial models. We are also studying the capture rate in high resolution galaxy models derived from cosmological n-body simulations where the galaxy is not necessarily in equilibrium; in this case, global potential fluctuations, triaxiality, and the occasional substructure merger can all play a role in replenishing the loss cone.

7 SUMMARY

At relatively large radii, a significant fraction of orbits in a triaxial galaxy stream so rapidly in angular momentum space that they replenish a loss cone as fast as it is depleted. Hence, we have shown that, in principle, loss cones in a triaxial galaxy may always be full at all energies. Nearly every orbit in a triaxial potential participates in this rapid angular momentum flow, reshuffling about 5% of the phase space content near r_{inf} over 1000 dynamical times, or on a timescale of 10^7 years for the Milky Way. Well inside r_{inf} the potential is rounder, and most orbits that make significant changes in angular momentum are chaotic. We found that the loss cone can be replenished through this process even deep in the potential, where the figure is nearly spherical.

When we consider angular momentum flow for orbits triaxial potential, we find that the capture rate is several orders of magnitude higher than spherical astrophysical capture estimates at nearly every radius. If our astrophysical white dwarf capture rate for the Milky Way of 10^{-5} per year is correct, it implies that up to 20% of our SMBH could have been grown from white dwarf accretion alone. We emphasize that the fractional number of white dwarfs accreted is still quite small: though about 25% of the white dwarf population passes through pericenter in a orbital time (by definition), only about 1 in 100000 are captured by the SMBH in our model.

Since dark matter halos are thought to be triaxial in shape, then if there is dark matter in galactic central cusps, this angular momentum flow can also move dark matter onto

an analogous, though much narrower, capture loss cone. Some estimates indicate that the density of dark matter dominates the stellar potential at 0.001 parsec (e.g. Bertone & Merritt 2005). If dark matter is less effective at scattering, particularly if it is not self-interacting, triaxiality may be an excellent mechanism to drive significant amounts of dark matter into the SMBH.

The capture and inspiral rate for an eternally full loss cone in a spherical galaxy has often been used as an upper limit, with the argument that a full loss cone cannot be more full. Note, however, that since triaxial galaxies have many more centrophilic orbits, the distribution function of a full triaxial loss cone can be 'supersaturated' compared to the full loss cone for a spherical isotropic galaxy. This could occur even the orbits were only able to change angular momentum via 2-body processes.

The surprisingly large replenishment rates imply large tidal disruption rates as well, since the tidal loss cone width is about 1000 times larger than the capture and inspiral loss cone. This suggests tidal disruption rates as high as 1×10^{-3} stars per year in a triaxial system with the same $\rho(r)$ as M32. In fact, this tidal disruption rate is consistent with what is inferred by the large amplitude X-ray outbursts observed at the centers of galaxies (Donley et al. 2002). Our inferred tidal disruption rate is rather large when our model is scaled to the Milky Way bar; however, it may be true that the angular momentum reshuffling process is less efficient in rotating bar potentials. Our numerical models also suggest that captures and tidal disruption events can originate from radii much larger than what is typically assumed; most centrophilic orbits in our model had apocenters much larger than 100 pc and though each centrophilic orbit contributes very little to the total rate, there are enough centrophilic orbits in our triaxial model to influence the capture or tidal disruption rate at large radii.

We have shown that triaxiality can increase the capture rate of single stars, but it may be even more important for binary systems. Binaries are funneled from large distances to the SMBH along centrophilic orbits in a triaxial galaxy. A close pericenter pass tidally separates the binary, with one member of the binary captured by the SMBH, and one ejected at high velocity. Since tidal separation can occur without significant energy loss, the typical captured star from a binary tidal separation can have an apocenter hundreds of times larger than a single stellar capture; this may make binary interactions a much more efficient capture mechanism (Miller et al. 2005), leading to a yet higher EMRI rate. In addition, the binary EMRI signal itself will be unique. When capture occurs at such large separations from the SMBH, there is ample time for the orbit to circularize by the time it becomes detectable by

LISA. Hence, there may be two classes of EMRI: the high eccentricity inspiral of a single star, and the zero eccentricity inspiral of a tidally separated binary. Comparing the ratio of the signals can probe the structure, stellar content, and recent kinematic history of the central regions of galaxies.

ACKNOWLEDGMENTS

We would like to acknowledge the support of the Center for Gravitational Wave Physics, which is funded by the National Science Foundation under the cooperative agreement PHY 01-14375. This work was completed with the support of a grant from the NSF, PHY 02-03046, and from NASA, ATP NNG04GU99G. This manuscript was written at the Aspen Center for Physics and KHB would also like to thank the Center and the other participants for their hospitality.

REFERENCES

- Bak, J., & Statler, T. 2000, *AJ*, 120, 110
- Bertone, G., & Merritt, D. 2005, astro-ph/054422
- Bogdanovic, T., Eracleous, M., Mahadevan, S., Sigurdsson, S., Laguna, P. 2004, *ApJ*, 610, 707
- Cohn, H., & Kulsrud, R. M. 1978, *ApJ*, 226, 1087
- Donley, J., Brandt, W., Eracleous, M., Boller, T. 2002, *AJ*, 124, 1308
- Diener, P., Kosovichev, A., Kotok, E., Novikov, I., Pethick, C. 1995, *MNRAS*, 275, 498
- Ferrarese, L., & Merritt, D. 2000, *ApJl*, 539, 9
- Frank, J., & Rees, M. 1976, *MNRAS*, 176, 633
- Franx, M., Illingworth, G., & de Zeeuw, T. 1991, *ApJ*, 383, 112
- Freitag, M. 2003, *ApJl*, 583, 21
- Gebhardt, K., Bender, R., Bower, G., Dressler, A., Faber, S. M., Filippenko, A., Green, R., Grillmair, C., Ho, L., Kormendy, J., Lauer, T., Magorrian, J., Pinkney, J., Richstone, D., Tremaine, S. 2000, *ApJl*, 539, 13
- Gebhardt, K., Pryor, C., O'Connell, R., Williams, T., Hesser, J. 2000, *AJ*, 119, 1268
- Gerhard, O.E., & Binney, J. 1985, *MNRAS*, 216, 467
- Gerhard, O.E. 2001, in ASP Conf. Se. 230, *Galaxy Disks and Disk Galaxies*, ed. J. G. Funes, S. J., & E. M. Corsini (San Francisco: ASP), 21

- Gerssen, J., van der Marel, R., Gebhardt, K., Guhathakurta, P., Peterson, R., & Pryor, C. 2003, *AJ*, 125, 376
- Ghez, A. M., Salim, S., Hornstein, S. D., Tanner, A., Lu, J. R., Morris, M., Becklin, E. E., Duchêne, G. 2005, *ApJ*, 620, 744
- Gould, A., & Quillen, A. 2003, *ApJ*, 592, 935
- Hils, D., & Bender, P. 1995, *ApJ*, 445, 7
- Hasan, D., & Norman, C. 1990, *ApJ*, 361, 69
- Hills, J. 1988, *Nature*, 331, 687
- Holley-Bockelmann, K., Mihos, J. C., Sigurdsson, S., Hernquist, L. 2001, *ApJ*, 549, 871
- Holley-Bockelmann, K., Mihos, J. C., Sigurdsson, S., Hernquist, L., & Norman, C. 2002, *ApJ*, 567, 817
- Hopman, C., & Alexander, T. 2005, *astro-ph/0503672*
- Ivanov, P. 2002, *MNRAS*, 336, 373
- Jogee, S., Barazza, F., Rix, H.-W., Shlosman, I., Barden, M., Wolf, C., Davies, J., Heyer, I., Beckwith, S., Bell, E., Borch, A., Caldwell, J., Conselice, C., Dahlen, T., Häussler, B., Heymans, C., Jahnke, K., Knapen, J., laine, S., Lubell, G., Mobasher, B., McIntosh, D., Meisenheimer, K., Peng, C., Ravindranath, S., Sanchez, S., Somerville, R., Wisotzki, L. 2004, *ApJl*, 615, 105
- Magorrian, J., & Tremaine, S. 1999, *MNRAS*, 309, 447
- Mapelli, M., Colpi, M., Possenti, A., & Sigurdsson, S. 2005, *astro-ph/0506405*
- Miller, C., & Hamilton, D. 2002, *MNRAS*, 330, 232
- Miller, C., Freitag, M., Hamilton, D., & Lauburg, V. 2005, *astro-ph/0507133*
- Milosavljevic, M., & Merritt, D. 2003, *ApJ*, 596, 860
- Miralda-Escude, J., & Schwarzschild, M. 1989, *ApJ*, 339, 752
- Merritt, D. & Quinlan, G. 1998, *ApJ*, 498, 625
- Merritt, D. & Poon, M. 2004, *ApJ*, 606, 788
- Norman, C.A., May, A., & van Albada, T.S. 1985, *ApJ*, 296, 20
- Peters, P. 1964, *Phys. Rev. B*, 136, 1224
- Peters, P. C., & Mathews, J. 1963, *Physical Review*, 131, 435
- Poon, M. & Merritt, D. 2002, *ApJ*, 568, 89
- Quinlan, G., Hernquist, L., & Sigurdsson, S. 1995, *ApJ*, 440, 554
- Rees, M. 1988, *Nature*, 333, 523
- Richstone, D., Ajhar, E., Bender, R., Bower, G., Dressler, A., Faber, S. M., Filippenko, A.,

- Gebhardt, K., Green, R., Ho, L., Kormendy, J., Lauer, T., Magorrian, J., Tremaine, S. 1998, *Nature*, 395, 14
- Scalo, J. 1986, *Fundamentals of Cosmic Physics*, vol. 11, p1
- Sellwood, J., & Shen, J. 2004, *ApJ*, 604, 614
- Sigurdsson, S., & Rees, M. 1997, *MNRAS*, 284, 318
- Sigurdsson, S. 1998, in *Proc. 2nd International LISA Symposium*, AIP Conf. Proc. 456, p 53 (AIP New York)
- Sheth, K., Menendez-Delmestre, K., Scoville, N., Jarrett, T., Strubbe, L., Regan, M., Schinnerer, E., Block, D. 2004, *astro-ph/0407322*
- Sridhar, S., & Tremaine, S. 1992, *Icarus*, 95, 86
- Taniguchi, Y., Shioya, Y., Tsuru, T., Ikeuchi, S. 2000, *PASJ*, 52, 533
- Valluri, M. & Merritt, D. 1998, *ApJ*, 506, 686
- Young, P. 1980, *ApJ*, 242, 1232
- Yu, Q., & Tremaine, S. 2003, *ApJ*, 599, 1129
- Zhao, H.-S., Haehnelt, M., & Rees, M. 2002, *NewA*, 7, 385